

taurex-emcee: automated, parallelized atmospheric retrievals with TauREx 3.1 and the emcee sampler

Andrea Bocchieri  ¹, **Quentin Changeat**  ², **Lorenzo V. Mugnai**  ^{3,4,5}, and **Enzo Pascale**  ¹

1 Department of Physics, La Sapienza Università di Roma, Piazzale Aldo Moro 2, Roma, 00185, Italy **2** European Space Agency (ESA), ESA Office, Space Telescope Science Institute (STScI), Baltimore, MD, 21218, USA **3** School of Physics and Astronomy, Cardiff University, Queens Buildings, The Parade, Cardiff, CF24 3AA, UK **4** Department of Physics and Astronomy, University College London, Gower Street, London, WC1E 6BT, UK **5** INAF, Osservatorio Astronomico di Palermo, Piazza del Parlamento 1, Palermo, I-90134, Italy

DOI: N/A

Software

- [Review](#) 
- [Repository](#) 
- [Archive](#) 

Editor: [Open Journals](#) 

Reviewers:

- [@openjournals](#)

Submitted: 01 January 1970

Published: 01 January 1970

License

Authors of papers retain copyright and release the work under a Creative Commons Attribution 4.0 International License ([CC BY 4.0](#)).

Summary

taurex-emcee is a plugin for the TauREx 3.1 atmospheric retrieval framework ([A. F. Al-Refaie et al., 2021](#)) that extends the choice of sampling methods available to the user. The plugin provides an interface to the `emcee` sampler ([Foreman-Mackey et al., 2013](#)), a popular affine-invariant ensemble sampler widely used in the astronomy community. Running the sampler to convergence is automated through the `autoemcee` package, which also supports parallelization with MPI. Thus, the taurex-emcee plugin allows users to easily launch parallelized retrievals of atmospheric spectra with emcee. This enables reliable, efficient, and fast retrievals, especially when coupled with TauREx's GPU-accelerated forward models ([A. Al-Refaie et al., 2020](#)).

taurex-emcee is released under the BSD 3-Clause license and is available on [GitHub](#). The plugin can be installed from the source code or from [PyPI](#), so it can be installed as `pip install taurex-emcee`. The documentation is available on [readthedocs](#), including a quick-start guide, a tutorial, a description of the software functionalities, and guidelines for developers. The documentation is continuously updated and is versioned to match the software releases.

Benchmark

We benchmarked the taurex-emcee plugin against the MultiNest sampler ([F. Feroz et al., 2009; Farhan Feroz et al., 2019](#)), natively implemented in TauREx 3, on a synthetic transmission spectrum of the hot Jupiter HD 209458b. The aim being first to assess the computational time of the two samplers on a controlled case, second to assess the consistency of the results from the retrievals. The synthetic spectrum and the retrievals were performed on a single node of the Sapienza University of Rome Melodie server, equipped with one NVIDIA A40 GPU. The high-resolution forward spectrum was generated assuming stellar and planetary parameters of HD 209458b from Edwards et al. (2019), reported in [Table 1](#).

Table 1: Summary of the selected target's properties.

R_p [R_J]	M_p [M_J]	T_p [K]	P [d]	R_s [R_\odot]	Mag K	T_s [K]	M_s [M_\odot]
1.35	0.71	1613	3.52	1.18	6.31	6,086	1.18

The stellar spectrum is simulated with the [Phoenix stellar models](#) ([Baraffe et al., 2015](#)), and the planetary atmosphere is gaseous, with hydrogen and helium at a ratio $H_2/He = 0.172$,

and has an isothermal temperature profile. We consider five molecular species as atmospheric trace gases: H₂O (100 ppm), CH₄ (10 ppm), CO (1 ppm), CO₂ (0.1 ppm), and NH₃ (0.01 ppm). Molecular abundances are assumed constant with altitude. We utilize cross sections at a resolution of 15,000 for all species, as given in [Table 2](#). Collision-induced absorption (CIA) with H₂–H₂ and H₂–He and Rayleigh scattering are included in the calculation. We also include fully-opaque gray clouds with a cloud-top pressure of 1000 Pa. Finally, 100 pressure layers are used to sample the atmosphere, from 1 Pa to 10⁶ Pa, uniformly in log-space.

Table 2: Cross sections and CIA used in the simulations.

Opacity	Reference(s)
H ₂ -H ₂	Abel et al. (2011), Fletcher et al. (2018)
H ₂ -He	Abel et al. (2012)
H ₂ O	Polyansky et al. (2018)
NH ₃	Coles et al. (2019)
CO	Li et al. (2015)
CO ₂	Rothman et al. (2010)
CH ₄	Yurchenko et al. (2017)

To simulate the observation of the transmission spectrum, we assume an observation by the Ariel space mission ([Tinetti et al., 2021, 2018](#)) in Tier 2 mode ([Edwards et al., 2019](#)). We utilize radiometric estimates of the total noise on one observation of HD 209458b obtained with ArielRad ([Mugnai et al., 2020](#)), the Ariel radiometric simulator now available at the online [exoddb.space](#) website. ArielRad is based on the generic point source radiometric model ExoRad2 ([Mugnai et al., 2023](#)), adapted with the Ariel payload configuration. The software versions used are: ExoRad2 v2.1.113, ArielRad-payloads v0.0.17, and ArielRad v2.4.26.

In our retrieval benchmarks, we attempt to constrain the abundances of the trace gases, alongside the temperature profile, the planetary radius, and the cloud-top pressure. [Table 3](#) lists each parameter, its units, and the priors (with corresponding scale) used in the retrievals.

Table 3: Parameters and priors used in the retrievals.

Parameter	Unit	Prior	Scale
R _P	R _J	±10%	linear
T	K	100; 4000	linear
H ₂ O	VMR	10 ⁻¹² ; 10 ⁻¹	log
CH ₄	VMR	10 ⁻¹² ; 10 ⁻¹	log
CO	VMR	10 ⁻¹² ; 10 ⁻¹	log
CO ₂	VMR	10 ⁻¹² ; 10 ⁻¹	log
NH ₃	VMR	10 ⁻¹² ; 10 ⁻¹	log
P _{clouds}	Pa	1; 10 ⁶	log

We perform five retrievals each with MultiNest and emcee, with increasing number of molecules included in the free parameters (the other molecules being fixed to their true values), from only H₂O to all five trace gases. With MultiNest, we set the evidence tolerance to 0.5 and sample the parameter space through 1500 live points. With emcee, we utilize 100 walkers and run two independent chains, each to convergence, where we adopt the default convergence criteria of the [autoemcee](#) package, i.e. the Geweke convergence diagnostic ([Geweke, 1991](#)) is z-score < 2.0 and the Gelman-Rubin rank diagnostic ([Gelman & Rubin, 1992](#)) is $\hat{r} < 1.01$. When iterating the chains, we increase the number of steps by multiplying the number of steps of the previous iteration by a growth factor of 2, a parameter that we have enabled as the

default value of 10 was deemed too conservative for our tests. As a first comparison, we report in [Table 4](#) the computational time of the retrievals with the two samplers.

Table 4: Runtime of the retrievals with emcee and MultiNest samplers.

Fitted molecules	Emcee [s]	MultiNest [s]
H_2O	16,465	5,423
$\text{H}_2\text{O}, \text{CH}_4$	6,550	7,505
$\text{H}_2\text{O}, \text{CH}_4, \text{CO}$	15,247	10,093
$\text{H}_2\text{O}, \text{CH}_4, \text{CO}, \text{CO}_2$	14,930	12,847
$\text{H}_2\text{O}, \text{CH}_4, \text{CO}, \text{CO}_2, \text{NH}_3$	30,151	17,097

MultiNest is faster than emcee for all the retrievals bar the one with H_2O and CH_4 , where the computational time is around 15 minutes longer. Additionally, runtimes with MultiNest scale slower with the increase in dimensionality of the parameter space. Finally, the first retrieval with emcee is slower than the second as the chains may require more iterations to converge based on the realization of the random walkers.

Next, we compare the results of the retrievals. For brevity, we only discuss the retrieval with the full stack of trace gases included in the free parameters, as the results of the other retrievals are consistent. [Figure 1](#) shows the retrieved spectrum yielded by the two samplers, alongside the observed spectrum. The retrieved spectrum is shown as the best-fit model and the 1σ and 2σ confidence intervals. The retrieved spectra are consistent with each other and with the observed spectrum within the experimental uncertainties.

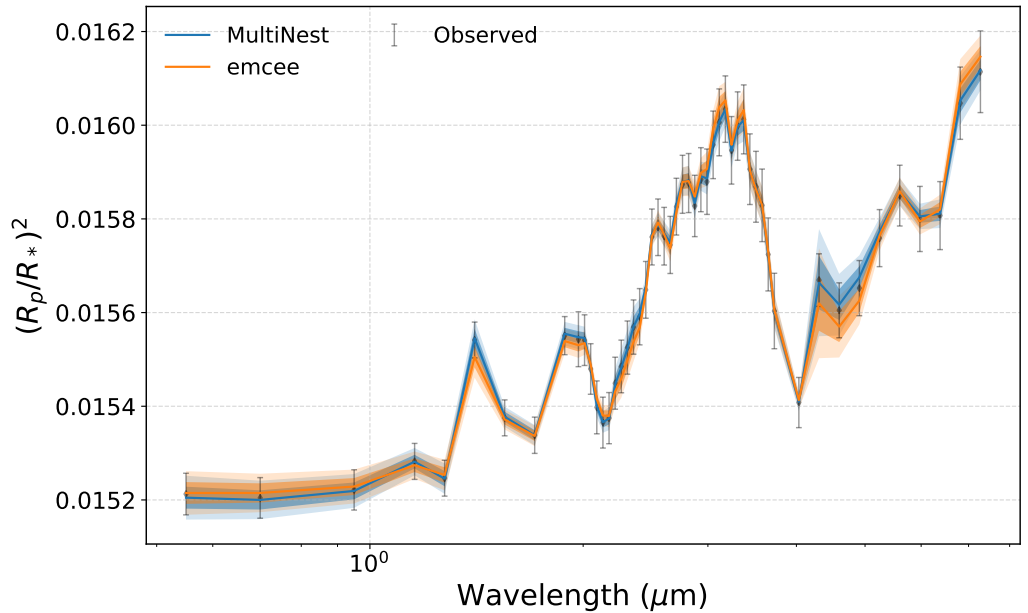


Figure 1: Best-fit spectra for the HD 209458b retrievals with MultiNest (blue) and emcee (orange). The synthetic observed spectrum is shown as the black error bars. The 1σ and 2σ confidence intervals are shown as the shaded regions. The error bars of the observed spectrum are generated with ArielRad ([Mugnai et al., 2020](#)) and the spectral grid corresponds to the Ariel Tier 2 mode ([Edwards et al., 2019](#)).

[Figure 2](#) shows the posteriors of the retrieved parameters, and [Table 5](#) reports the median and 16% and 84% quantiles of the marginalized posteriors relative to the median.

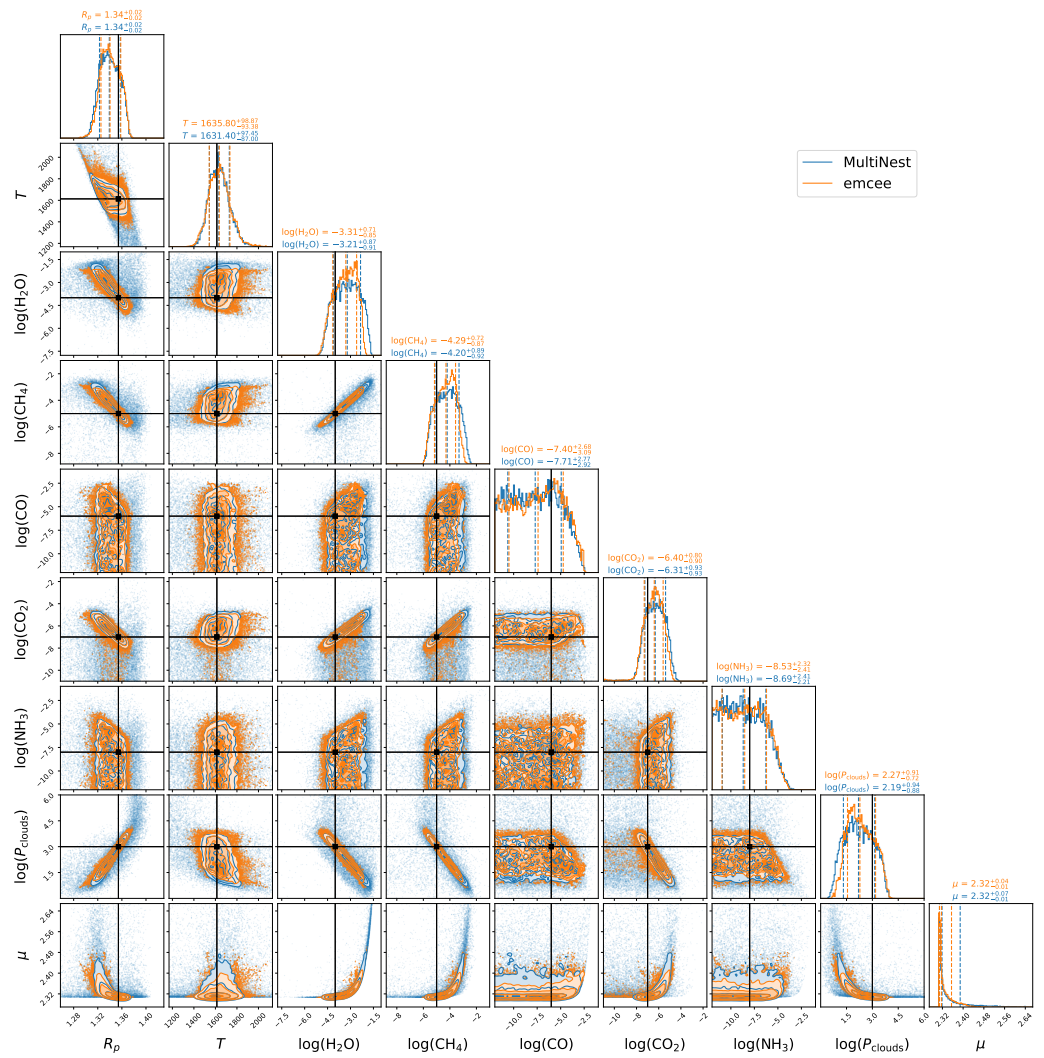


Figure 2: Posterior distributions of the retrieved parameters for the HD 209458b simulated observations with MultiNest (blue) and emcee (orange). The true values are shown as the vertical black lines. The vertical dashed lines in the histograms on the diagonal show the median and 16% and 84% quantiles.

Table 5: Retrieved parameters and their uncertainties. True values are reported for comparison.

Parameter	True value	Emcee	MultiNest
R_p	1.35	$1.34^{+0.02}_{-0.02}$	$1.34^{+0.02}_{-0.02}$
T	1613	$1635.8^{+98.9}_{-93.4}$	$1631.4^{+97.5}_{-87.0}$
$\log(H_2O)$	-4	$-3.31^{+0.71}_{-0.85}$	$-3.21^{+0.87}_{-0.91}$
$\log(CH_4)$	-5	$-4.29^{+0.72}_{-0.87}$	$-4.20^{+0.89}_{-0.92}$
$\log(CO)$	-6	$-7.4^{+2.7}_{-3.1}$	$-7.7^{+2.8}_{-2.9}$
$\log(CO_2)$	-7	$-6.40^{+0.80}_{-0.90}$	$-6.31^{+0.93}_{-0.93}$
$\log(NH_3)$	-8	$-8.5^{+2.3}_{-2.4}$	$-8.7^{+2.4}_{-2.2}$
$\log(P_{clouds})$	3	$2.27^{+0.91}_{-0.72}$	$2.19^{+0.94}_{-0.88}$
μ		$\mu = 2.32^{+0.01}_{-0.01}$	$\mu = 2.32^{+0.01}_{-0.01}$

The similarity of the results from the two samplers is reassuring, and the retrieved parameters are consistent with the true values within 1σ . It is worth noting that the median values are, to an extent, biased for both samplers, in essentially the same manner. This result is expected,

as the retrieval traces the degeneracies between the parameters and the fitted molecules have strong correlations with each other, as seen in Figure 2. In addition, for some parameters, namely CO and NH₃, due to the combination of opacities and abundances, the retrievals only recover an upper limit. In these cases, mean, median, and mode are not defined, and the reported values depend on the choice of the prior.

In summary, while the emcee sampler is generally slower than MultiNest, it is a robust and reliable alternative to nested samplers, as shown by the consistency of the results from the two samplers in our benchmark.

Statement of need

Optimized sampling methods are a key component of any retrieval code. Nested samplers (F. Feroz et al., 2009; Farhan Feroz et al., 2019) are a powerful and robust sampling method, successfully applied to the retrieval of exoplanet atmospheric spectra (Barstow et al., 2020; Bocchieri et al., 2023; Changeat et al., 2020). TauREx 3.1 natively implements a suite of nested samplers, including the MultiNest sampler, or makes them available as plugins, such as the UltraNest sampler. The primary target of nested samplers is the efficient calculation of the Bayesian evidence, whilst the inference of the posterior is a by-product. This is regarded as a key advantage of nested samplers, as the evidence can be readily used for model selection. However, the evidence is not always required, and the interpretation of the posterior from nested samplers necessitates some care. Additionally, algorithmic assumptions of nested samplers may require to tailor the priors to explore the parameter space thoroughly.

Where the inference of the Bayesian posterior is the primary target, a well-established alternative to nested samplers are a family of Markov chain Monte Carlo methods known as affine-invariant ensemble samplers (Goodman & Weare, 2010). The implementation in emcee (Foreman-Mackey et al., 2013) is a popular choice in the astronomy community, as it takes care of the heavy lifting of the sampling process, is well documented, and is straightforward to utilize. To date, the emcee sampler is not natively implemented in the TauREx 3.1 retrieval framework, nor elsewhere in other retrieval codes, to the knowledge of the authors. To fill this gap, we developed the taurex-emcee plugin, which interfaces the emcee sampler to TauREx. Key advantages of taurex-emcee are that it affords a more straightforward interpretation of the posterior and is more robust to the choice of priors. However, the current implementation is not intended to explore multimodal posteriors, for which nested samplers will inevitably be more efficient. Moreover, we caveat that it may require substantial computational time to sample high-dimensional parameter spaces with emcee, which can be mitigated by coupling taurex-emcee with TauREx's GPU-accelerated forward models (A. Al-Refaie et al., 2020).

Acknowledgements

This work was supported by the Italian Space Agency (ASI) with Ariel grant n. 2021.5.HH.0.

References

- Abel, M., Frommhold, L., Li, X., & Hunt, K. L. C. (2011). Collision-induced absorption by H₂ pairs: From hundreds to thousands of kelvin. *The Journal of Physical Chemistry A*, 115(25), 6805–6812. <https://doi.org/10.1021/jp109441f>
- Abel, M., Frommhold, L., Li, X., & Hunt, K. L. C. (2012). Infrared absorption by collisional H₂-He complexes at temperatures up to 9000 k and frequencies from 0 to 20,000 cm(-1). *The Journal of Chemical Physics*, 136(4), 044319. <https://doi.org/10.1063/1.3676405>
- Al-Refaie, A. F., Changeat, Q., Waldmann, I. P., & al., et. (2021). TauREx 3: A Fast, Dynamic, and Extendable Framework for Retrievals. 917(1), 37. <https://doi.org/10.3847/>

[1538-4357/ac0252](#)

- Al-Refaie, A., Changeat, Q., Venot, O., & al., et. (2020). TauREx 3.1 - Extending atmospheric retrieval with plugins. *European Planetary Science Congress*, EPSC2020–669. <https://doi.org/10.5194/epsc2020-669>
- Baraffe, I., Homeier, D., Allard, F., & al., et. (2015). New evolutionary models for pre-main sequence and main sequence low-mass stars down to the hydrogen-burning limit. 577, A42. <https://doi.org/10.1051/0004-6361/201425481>
- Barstow, J. K., Changeat, Q., Garland, R., & al., et. (2020). A comparison of exoplanet spectroscopic retrieval tools. 493(4), 4884–4909. <https://doi.org/10.1093/mnras/staa548>
- Bocchieri, A., Mugnai, L. V., Pascale, E., & al., et. (2023). Detecting molecules in Ariel low resolution transmission spectra. *Experimental Astronomy*, 56(2-3), 605–644. <https://doi.org/10.1007/s10686-023-09911-x>
- Changeat, Q., Al-Refaie, A., Mugnai, L. V., & al., et. (2020). Alfnoor: A Retrieval Simulation of the Ariel Target List. 160(2), 80. <https://doi.org/10.3847/1538-3881/ab9a53>
- Coles, P. A., Yurchenko, S. N., & Tennyson, J. (2019). ExoMol molecular line lists - XXXV. A rotation-vibration line list for hot ammonia. 490(4), 4638–4647. <https://doi.org/10.1093/mnras/stz2778>
- Edwards, B., Mugnai, L., Tinetti, G., & al., et. (2019). An Updated Study of Potential Targets for Ariel. 157(6), 242. <https://doi.org/10.3847/1538-3881/ab1cb9>
- Feroz, F., Hobson, M. P., & Bridges, M. (2009). MULTINEST: an efficient and robust Bayesian inference tool for cosmology and particle physics. 398(4), 1601–1614. <https://doi.org/10.1111/j.1365-2966.2009.14548.x>
- Feroz, Farhan, Hobson, M. P., Cameron, E., & al., et. (2019). Importance Nested Sampling and the MultiNest Algorithm. *The Open Journal of Astrophysics*, 2(1), 10. <https://doi.org/10.21105/astro.1306.2144>
- Fletcher, L. N., Gustafsson, M., & Orton, G. S. (2018). Hydrogen Dimers in Giant-planet Infrared Spectra. 235(1), 24. <https://doi.org/10.3847/1538-4365/aaa07a>
- Foreman-Mackey, D., Hogg, D. W., Lang, D., & al., et. (2013). emcee: The MCMC Hammer. 125(925), 306. <https://doi.org/10.1086/670067>
- Gelman, A., & Rubin, D. B. (1992). Inference from Iterative Simulation Using Multiple Sequences. *Statistical Science*, 7, 457–472. <https://doi.org/10.1214/ss/1177011136>
- Geweke, J. (1991). *Evaluating the accuracy of sampling-based approaches to the calculation of posterior moments* (Staff Report No. 148). Federal Reserve Bank of Minneapolis. <https://ideas.repec.org/p/fip/fedmsr/148.html>
- Goodman, J., & Weare, J. (2010). Ensemble samplers with affine invariance. *Communications in Applied Mathematics and Computational Science*, 5(1), 65–80. <https://doi.org/10.2140/camcos.2010.5.65>
- Li, G., Gordon, I. E., Rothman, L. S., & al., et. (2015). Rovibrational Line Lists for Nine Isotopologues of the CO Molecule in the X $^1\Sigma^+$ Ground Electronic State. 216(1), 15. <https://doi.org/10.1088/0067-0049/216/1/15>
- Mugnai, L. V., Bocchieri, A., & Pascale, E. (2023). ExoRad 2.0: The generic point source radiometric model. *The Journal of Open Source Software*, 8(89), 5348. <https://doi.org/10.21105/joss.05348>
- Mugnai, L. V., Pascale, E., Edwards, B., & al., et. (2020). ArielRad: the Ariel radiometric model. *Experimental Astronomy*, 50(2-3), 303–328. <https://doi.org/10.1007/s10686-020-09676-7>

- Polyansky, O. L., Kyuberis, A. A., Zobov, N. F., & al., et. (2018). ExoMol molecular line lists XXX: a complete high-accuracy line list for water. *480*(2), 2597–2608. <https://doi.org/10.1093/mnras/sty1877>
- Rothman, L. S., Gordon, I. E., Barber, R. J., Dothe, H., Gamache, R. R., Goldman, A., Perevalov, V. I., Tashkun, S. A., & Tennyson, J. (2010). HITEMP, the high-temperature molecular spectroscopic database. *111*, 2139–2150. <https://doi.org/10.1016/j.jqsrt.2010.05.001>
- Tinetti, G., Drossart, P., Eccleston, P., & al., et. (2018). A chemical survey of exoplanets with ARIEL. *Experimental Astronomy*, *46*(1), 135–209. <https://doi.org/10.1007/s10686-018-9598-x>
- Tinetti, G., Eccleston, P., Haswell, C., & al., et. (2021). Ariel: Enabling planetary science across light-years. *arXiv e-Prints*, arXiv:2104.04824. <https://doi.org/10.48550/arXiv.2104.04824>
- Yurchenko, S. N., Amundsen, D. S., Tennyson, J., & al., et. (2017). A hybrid line list for CH₄ and hot methane continuum. *605*, A95. <https://doi.org/10.1051/0004-6361/201731026>